Inorg. Chem. **1994**, *33*, 2586–2591

Carbon Number Dependence of the Intercalation and Interlayer Amidation Properties of α,ω-Alkylidiamines for Layered Zirconium (Carboxyethyl)phosphonate

Tsuyoshi Kijima,* Shinichi Watanabe, and Masato Machida

Department of Materials Science, Faulty of Engineering, Miyazaki University, Miyazaki 889-21, Japan

Received December 14, 1993[⊛]

A striking dependence on carbon number of the intercalation and interlayer amidation properties of α,ω-alkyldiamines $H_2N(CH_2)_nNH_2$ ($n = 2$–10) has been found for layered zirconium (carboxyethyl)phosphonate. Each alkyldiamine forms one or two intercalated phases in which the diamine molecules are arranged as a monolayer with their two ammonium termini binding to the carboxyl groups of any two adjacent phosphonate layers. The interlayer spacing vs n plots for the intercalated solids indicate that the axes of molecules in the monolayer are tilted by 19 or 59° relative to the inorganic layer to form two groups of intercalates. Diamine with $n \leq 7$ show a tendency to produce the high and low chain-tilt forms depending on the even and odd numbers of carbon atoms, respectively, but both forms coexist for $n = 4$, 6, and 7. For diamines with longer chain lengths, on the other hand, only the high chain-tilt form is observed. Upon heating at 120 °C or above, all the diammonium-exchanged solids are condensed into their amide-functionalized forms, accompanying a partial desorption of the amine guests. The amidated phases are grouped into high and low chain-tilt forms depending only on the carbon chain length. The amidation also leads to an interlayer contraction of ca. 1.5 Å for the high chain-tilt form, but a slight interlayer expansion occurs for the other form. With an increase of the carbon number n, the temperature for the amidation to begin increases regularly up-and-down depending on the even or odd character of n.

Introduction

Increasing attention has been paid to layered metal organo phosphates and organophosphonates which have various useful functions including ion exchange,[1] ionic conduction,[1a,2] molecular recognition,[3] and catalysis.[4] Such organo derivatives widely range from the most familar tetravalent metal (Zr, Ti, Hf, Ce, Th) phosphates and phosphonates to vanadyl phosphonates,[3,5] divalent metal (Mg, Ca, Mn, Zn, Cd) phosphonates,[6] and trivalent metal (La, Sm, Ce, Fe) phosphonates.[7]

Layered zirconium organo phosphates were first synthesized by Yamanaka in 1976 by the replacement of the interlayer HPO_4^{2-} groups of γ-zirconium phosphate with various organo phosphoric ester ions.[8] In 1978, Alberti et al. reported the synthesis of a more attractive family of layered tetravalent metal phosphates and phosphonates given by the general formulas $M(O_3POR)_2$ and $M(O_3PR)_2$, respectively.[9] These compounds can be obtained by the direct reaction of tetravalent metal ions with organo phosphoric or organophosphonic acids in the presence of hydrofluoric acid. This method was applied by Alberti et al.,[9,10] by Maya,[11] and by Dines and co-workers[12] to the preparation of a broad range of teravalent metal phosphates and phosphonates containing organic groups such as alkyl, phenyl, COOH, and SO_3H. The tetravalent metal phosphates and phosphonates thus obtained have essentially the same layered structure as α-$Zr(HPO_4)_2{\cdot}H_2O$ (α-ZrP).[13] Each layer consists of a plane of metal atoms linked through phosphate or phosphonate groups located alternately above and below this plane. The three oxygen atoms of each tetrahedral phosphate or phosphonate group bond to three different meal atoms, forming an octahedron about each metal atom, and the organic functional group (OR or R) points toward an adjacent layer in the structure.

Recently, Burwell and Thompson reported the synthesis of a new class of layered zirconium phosphonates containing amide and ester linkages.[14] These compounds were obtained by the intercalation reactions of the Lewis acidic layered compound $Zr(O_3PCH_2CH_2COCl)_2$ with amines and alcohols, preceded by the preparation of the acyl chloride via the reaction of the ammonium intercalate of $Zr(O_3PCH_2CH_2COOH)_2$ with thionyl chloride. More recently, on the other hand, we found that a similar amide-functionalized zirconium phosphonate can be obtained by the thermal condensation of the ethylenediammonium-exchanged form of partially orthophosphated zirconium (carboxyethyl)-phosphonate $Zr(O_3PCH_2CH_2COOH)_{1.67}(HPO_4)_{0.33}$ at ca. 200 °C.[15] This finding is worthwhile in that it opened a simple route to amide derivatives of metal phosphonates from their carboxylic acid forms without preparatory conversion of the acid groups to

---

[⊛] Abstract published in *Advance ACS Abstracts,* May 1, 1994.

(1) (a) Alberti, G.; Casciola, M.; Costantino, U.; Fabrani, D. In *Membranes and Membrane Processes*; Drioli, E., Nakagaki, M., Eds.; Plenum Publishing Corp.: New York, 1986. (b) Clearfield, A. *Chem. Rev.* **1988**, *88*, 125.

(2) (a) Alberti, G.; Costantino, U.; Casciola, M.; Vivani, R. *Solid State Ionics* **1991**, *46*, 61. (b) Casciola, M.; Chieli, S.; Costantino, U.; Peraio, A. *Solid State Ionics* **1991**, *46*, 53.

(3) Jhonson, J. W.; Jacobson, A. J.; Butler, W. M.; Rosenthal, S. E.; Brody, J. F.; Lewandowski, J. T. *J. Am. Chem. Soc.* **1989**, *111*, 381.

(4) (a) Alberti, G.; Costantino, U. *J. Mol. Catal.* **1994**, *27*, 235. (b) Vermeulen, L. A.; Thompson, M. E. *Nature* **1992**, *358*, 656.

(5) (a) Johnson, J. W.; Jacobson, A. J.; Brody, J. F.; Lewandowski, J. T. *Inorg. Chem.* **1984**, *23*, 3842. (b) Huan, G.; Jacobson, A. J.; Johnson, J. W.; Corcoran, E. W., Jr. *Chem. Mater.* **1990**, *2*, 91. (c) Johnson, J. W.; Brody, J. F.; Alexander, R. M.; Pilarski, B.; Katritzky, A. R. *Chem. Mater.* **1990**, *2*, 198.

(6) (a) Cao, G.; Lee, H.; Lynch, V. M.; Mallouk, T. E. *Inorg. Chem.* **1988**, *27*, 2781. (b) Cao, G.; Lee, H.; Lynch, V. M.; Mallouk, T. E. *Solid State Ionics* **1988**, *26*, 63. (c) Ortiz-Avila, C. Y.; Rudolf, P. R.; Clearfield, A. *Inorg. Chem.* **1989**, *28*, 2137.

(7) (a) Cao, G.; Lynch, V. M.; Swinnea, J. S.; Mallouk, T. E. *Inorg. Chem.* **1990**, *29*, 2112. (b) Bujoli, B.; Palvadeau, P.; Rouxel, J. *Chem. Mater* **1990**, *2*, 582.

(8) Yamanaka, S. *Inorg. Chem.* **1976**, *15*, 2811.

(9) Alberti, G.; Costantino, U.; Alluilli, S.; Tomassini, N. *J. Inorg. Nucl. Chem.* **1978**, *40*, 1113.

(10) (a) Alberti, G.; Costantino, U.; Giovagnotti, M. L. L. *J. Chromatogr.* **1979**, *180*, 45. (b) Alberti, G.; Costantino, U.; Kornyei, J.; Giovagnotti, M. L. L. *React. Polym.* **1985**, *4*, 1.

(11) Maya, L. *Inorg. Nucl. Chem. Lett.* **1979**, *15*, 207.

(12) (a) Dines, M. B.; Digiacomo, P. M. *Inorg. Chem.* **1981**, *20*, 92. (b) Digiacomo, P. M.; Dines, M. B. *Polyhedron* **1982**, *1*, 61. (c) Dines, M. B.; Griffith, P. C. *Polyhedron* **1983**, *2*, 607. (d) Dines, M. B.; Griffith, P. C. *Inorg. Chem.* **1983**, *22*, 567. (e) Dines, M. B.; Cooksey, R. E.; Griffith, P. C.; Lane, R. H. *Inorg. Chem.* **1983**, *22*, 1003.

(13) Alberti, G.; Costantino, U. In *Intercalation Chemistry*; Whittingham, M. S., Jacobson, A. J., Eds.; Academic Press: New York, 1982.

(14) (a) Burwell, D. A.; Thompson, M. E. *Chem. Mater.* **1991**, *3*, 14. (b) Burwell, D. A.; Thompson, M. E. *Chem. Mater.* **1991**, *3*, 730.

(15) Kijima, T.; Kawagoe, Y.; Mihara, K.; Machida, M. *J. Chem. Soc., Dalton Trans.* **1993**, 3827.

0020-1669/94/1333-2586\$04.50/0

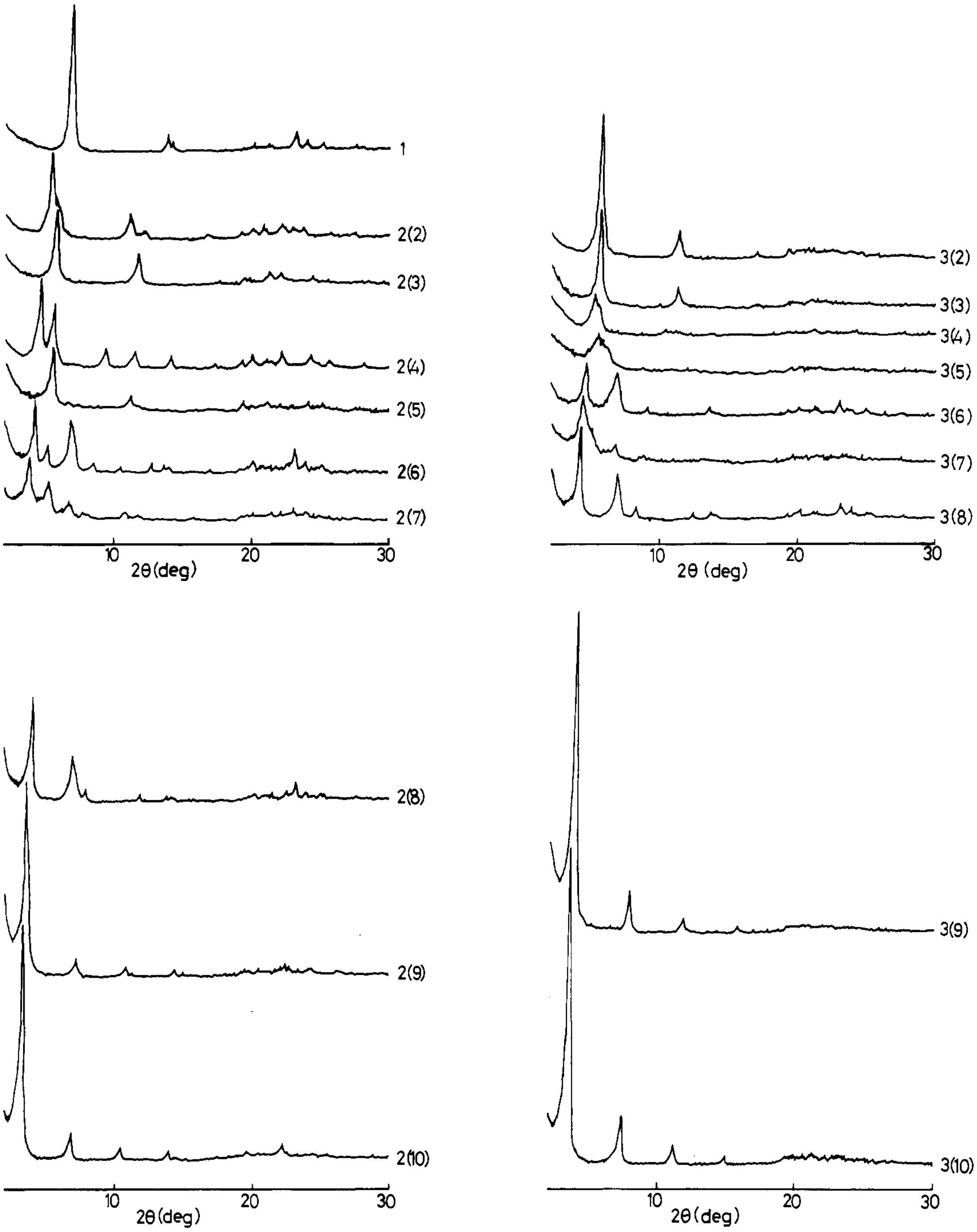

Figure 1. X-ray diffraction patterns of (A, left) **1** and **2**(*n*) and (B, right) **3**(*n*).

Table 1. Interlayer Spacing and Composition as a Function of the Carbon Number of Diamine, *n*, for the Diammonium-Exchanged Form of **1** Prepared by Precipitation at the Reactant Ratio [diamine]/[Zr] = 1.0, **2**(*n*), and the Amide Form Prepared by Heating **2**(*n*) at 210 °C for 1 h, **3**(*n*)

	diammonium form, **2**(*n*), $Zr(O_3PC_2H_4COOH)_{1.67}(HPO_4)_{0.33}(H_2NC_nH_{2n}NH_2)_x{\cdot}yH_2O$				diamide form, **3**(*n*), $Zr(O_3PC_2H_4COOH)_{1.67-2x}(HPO_4)_{0.33}(O_3PC_2H_4CONHC_nH_{2n}NHCOH_4C_2PO_3)_x{\cdot}yH_2O$		
n	interlayer spacing/Å		*x*	*y*	interlayer spacing/Å	*x*	*y*
2	16.1		0.62	0.47	15.7	0.58	0.57
3	15.4		0.23	0.58	15.8	0.10	0.56
4	18.9	15.7	0.70	0.0	16.7	0.61	0.0
5	16.0		0.38	0.81	16.5	0.34	0.57
6	21.2	17.2	0.21	0.0	19.6	0.19	0.0
7	22.2	16.7	0.36	0.43	20.4	0.35	0.29
8	23.2		0.41	0.0	21.6	0.38	0.0
9	23.9		0.72	0.23	22.6	0.71	0.0
10	25.0		0.74	0.0	23.9	0.74	0.0

acyl chlorides. Moreover, our observations appear to be in contrast to the previous reports[14b,16] that the alkylmonoaminated forms of the carboxy-terminated zirconium phosphonate, $Zr(O_3PCH_2CH_2COO^-)_2(RNH_3^+)_2$, release the amine guest upon heating at temperatures of ca. 200 °C. Therefore, the thermal amidation method must be studied in more detail, including its applicability to other guest compounds.

An attempt was thus made to investigate the intercalation of α,ω-alkyldiamines $H_2N(CH_2)_nNH_2$ (n = 2–10) in zirconium (carboxyethyl)phosphonate and the subsequent interlayer ami-

Table 2. Orientations of the Carbon Chain Axes and Planes for the High and Low Chain-Tilt Groups of the Diammonium and Diamide Forms in the 1-Alkyldiamine System and Those for the Diammonium Form of α-ZrP

	1-alkyldiamine system				
	diammonium form		diamide form		
	low tilt	high tilt	low tilt	high tilt	diammonium form of α-ZrP[a]
d–*n* relation	$0.41n + 14.2$	$1.09n + 14.3$	$0.33n + 15.0$	$1.02n + 13.6$	$1.08n + 8.93$
θ/deg	19	59	15	53	58
θ_0/deg		49		64	55
ω_0/deg		80		72	58
Δd_1/Å		+1.05		+1.25	+1.3
Δd_2/Å		+0.85		+1.0	+0.75

[a] Calculated using data given in ref 17.

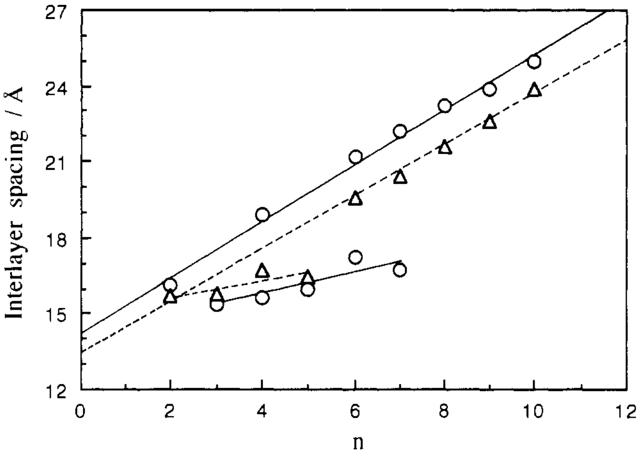

Figure 2. Interlayer spacings of (○) **2**(*n*) and (△) **3**(*n*) versus carbon number of alkyl chain.

dation. The present paper describes the validity of the thermal amidation method for a family of alkyldiamines, along with the carbon number dependence of the diammonium intercalation and subsequent amidation properties.

Experimental Section

Reagents. The zirconium (carboxyethyl)phosphonate sample used in this study was prepared in a manner similar to that of Alberti et al.[9] Concentrated hydrofluoric acid and 31.6 mmol (4.87 g) of $HOOCC_2H_4PO(OH)_2$ were added to 200 dm^3 of a 5.25×10^{-2} mol dm^{-3} aqueous solution of $ZrOCl_2$. The reaction mixture with the ratios [P]/[Zr] = 3.0 and [F]/[Zr] = 5.0 was stirred at 90 °C for 10 days while the hydrofluoric acid was allowed to evaporate spontaneously into a chilled trap. The reaction product was filtered off, washed with water to pH 3, and then freeze-dried. The thermogravimetric curve up to 1000 °C for the resulting solid showed no weight loss other than that of 29.6% observed in the temperature range 280–700 °C. On heating at 1000 °C for 1 h, the solid was totally converted into ZrP_2O_7. On the basis of these data, the composition of the zirconium (carboxyethyl)phosphonate sample was determined to be $Zr(PO_3C_2H_4COOH)_{1.67}(HPO_4)_{0.33}$ (**1**). The C and H contents of this sample were 16.5 and 2.6 wt % with an error of ±0.5%, in accordance with 16.0 and 2.3% evaluated from the thermogravimetrically determined composition. These analytical results indicate that the (carboxyethyl)phosphonate used has partially hydrolyzed during the reaction with $ZrOCl_2$ in an aqueous solution to form P–OH groups. The formation of orthophosphate ions was qualitatively confirmed by the coloration of the supernatant solution with ammonium molybdate.

Ion-Exchange Reaction. A 0.05-g sample of **1** was accurately mixed with 5 cm^3 of aqueous alkyldiamine solution at a fixed ratio of [amine]/[Zr] = 1.0, followed by stirring at 25 °C for 10 days. The [amine]/[Zr] ratio of 1.0 was selected because some representative systems including ethylenediamine[15] had shown an increasing tendency for the host phase **1** to partially decompose at higher amine concentrations. The equilibration time of 10 days was employed after preliminary experiments had shown invariant pH for longer times. The resulting mixtures were centrifuged, fully washed with water, and freeze-dried. The pH of the supernatants was measured by a TOA Model TSC-10A autotitrator.

Sample Characterization. Thermogravimetry was carried out with a Shinku Riko instrument at a heating rate of 10 °C min^{-1} in air. Elemental C and H analysis was conducted using a Yanako Model MT-3 CHN corder. X-ray diffraction measurements were made on a Shimazu diffractometer with Cu Kα radiation using tetradecan-1-ol as an external standard. Infrared (IR) absorption spectra were measured by the KBr-pellet method using a Hitachi Model 270–30 spectrometer.

Results and Discussion

As shown in Figure 1A, the X-ray diffraction patterns of **1** and its reaction products with alkyldiamines, **2**(*n*), are characterized by the major peaks at 2θ = ca. 3.5–6.8° attributable to the (002) reflections, along with their second- and/or third-order reflections. The X-ray data indicate that 1,2-diaminoethane (EDA; $n = 2$), 1,3-diaminopropane (PrDA; $n = 3$), 1,5-diaminopentane (PeDA; $n = 5$), 1,8-diaminooctane (OcDA; $n = 8$), 1,9-diaminononane (NoDA; $n = 9$), and 1,10-diaminodecane (DeDA; $n = 10$) form one intercalated phase, whereas 1,4-diaminobutane (BuDA; $n = 4$), 1,6-diaminohexane (HeDA; $n = 6$), and 1,7-diaminoheptane (HpDA; $n = 7$)) form two intercalated phases with different interlayer spacings. For the reaction solids with HeDA, HpDA, and OcDA, some portion of the host phase **1** remains unreacted. The interlayer spacings of the intercalated phases observed were determined from the first and/or second maximum *d* value in the X-ray diffraction patterns (Table 1). The plots of interlayer spacing (*d*) in angstroms against the number of CH_2 units (*n*) in the alkyl chain yield two straight lines with high and low slopes (Figure 2). The slopes of these lines evaluated from data for n = 2, 4, 6–10 and those for n = 3–7 are 1.09 and 0.41, respectively, and these values are less than a typical methylene repeat distance of 1.27 Å/CH_2 for an all-trans polymethylene chain. These observations indicate the formation of two groups of intercalated phases with average angles (θ) of orientation between the carbon chains and the layer of 19 and 59° (Table 2). There is a general tendency that diamines with $n \leq 7$ produce the high and low chain-tilt forms depending upon the even and odd numbers of carbon atoms, respectively, whereas longer chain diamines yield only the high chain-tilt form. Both forms coexist for intermediate members with *n* of 4, 6, and 7. The $Zr(O_3PC_2H_4COOH)_2$–alkylmonoamine system also yielded two similar groups of intercalates with different chain orientations,[16] for which the two slopes of 1.1 and 2.2 Å/CH_2 are about 2 times higher than those observed for the present system. The extremely sharp peaks of X-ray diffraction for the NoDA and DeDA intercalates suggest that the phosphonate and intercalant layers are highly ordered, due to enhanced intermolecular attraction of the diamine guests.

The IR absorption spectra of the diamine-intercalated solids showed that the absorption peak at 1710 cm^{-1} due to the C=O stretching of the –COOH group observed for **1** decreases in intensity or disappears upon addition of alkyldiamines, whereas a new broad band attributable to the $-COO^-NH_3^+-$ group appears near 1680 cm^{-1} (Figure 3A). This indicates that the intercalation of alkyldiamine molecules proceeds by a mode in which the $-NH_3^+$ termini of their diammonium-exchanged forms replace the protons of the interlayer COOH groups to yield an ionically bonded $-COO^-NH_3^+-$ form. The remaining 1710-cm^{-1} bands for **2**(**8**),

---

[16] Kornyei, J.; Szirtes, L.; Costantino, U. *J. Radioanal. Nucl. Chem.* **1985**, *89*, 331.

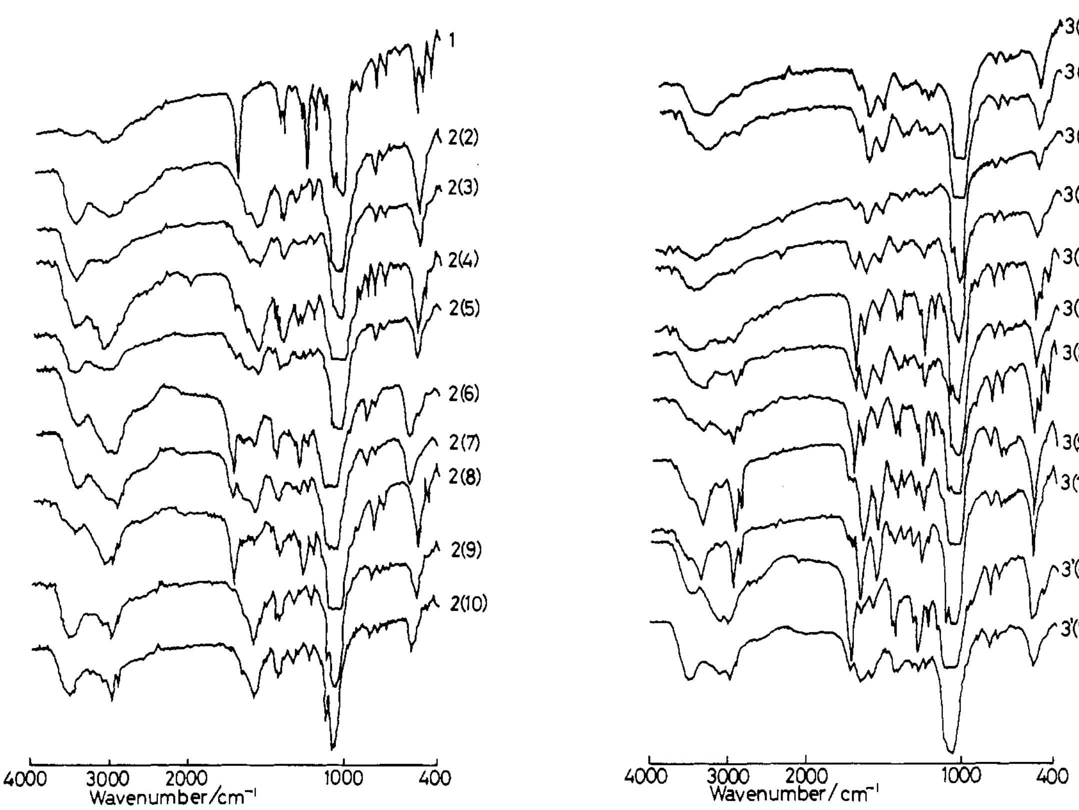

Figure 3. Infrared spectra of (A, left) **1** and **2**(*n*) and (B, right) **3**(*n*), **3'**(**6**), and **3'**(**7**). Samples **3'**(**6**) and **3'**(**7**) are **3**(**6**) and **3**(**7**) heated at 180 and 160 °C, respectively, for 10 min.

2(**6**), and **2**(**7**) are in accord with the X-ray observations indicating the lesser reactivities of OcDA, and HpDA with the host phase **1** in that order compared to those of the other diamines.

When the diammonium-exchanged solids were heated at 210 °C for 1 h, the IR absorption band near 1680 cm^{-1} due to the $-COO^-NH_3^+-$ group was almost totally converted into so-called amide-I and -II bands at 1655 and 1560 cm^{-1}, respectively (n = 2–4, 8–10), or partly recovered into the initial –COOH band at 1710 cm^{-1} (n = 5–7) (Figure 3B). The two amide bands for the pyrolyzed products **3**(*n*) are similar to those at 1646 and 1548 cm^{-1} observed for alkaneamide intercalation compounds of zirconium phosphonate derived from the acyl chloride form.[14] The above IR observations indicate that the interlayer ionically bonded $-COO^-NH_3^+-$ group in the diammonium-exchanged solids is thermally condensed into the amide –CONH– form accompanying a partial deintercalation of the diamine guests to leave the regenerated acid host. The deintercalation of intercalated diamine is marked for PeDA, HeDA, and HpDA. The X-ray diffraction patterns for the amidated solids are shown in Figure 1B, and the interlayer spacings are listed in Table 1, including approximate values for n = 4, 5, and 7 obtained from the peak positions of their broad (002) reflections. In contrast to those for the diammonium-exchanged phases, the d vs n plots for the amidated phases yield two straight lines depending only on the carbon chain length, one for n = 6–10 and the other for n = 2–5 (Figure 2). The slopes of these two lines are 1.02 and 0.33, which indicate average angles of orientation between the carbon chains and the phosphonate layer of 53 and 15°, respectively (Table 2). It is also noted that the amidation causes an interlayer contraction of ca. 1.5 Å for the high chain-tilt form, due to thermal condensation, whereas a slight interlayer expansion occurs for the other form.

The thermogravimetric curves for the diammonium-exchanged solids **2**(*n*) indicated two or three steps over the temperature range 0–700 °C, as shown in Figure 4. The first weight loss at below 100 °C is due to the desorption of interlayer water, and this weight loss is characteristic of the solids with odd carbon numbers, except for **2**(**2**). The second weight loss in the 100–250 °C temperature range, observed for all the diammonium-exchanged solids, is attributable to the conversion of the ionically bonded $-COO^-NH_3^+-$ group into the amide –CONH– form, accompanied by partial deintercalation of the intercalated amine, as suggested from the above IR observations. The third weight loss at above 300 °C is primarily due to a loss of the interlayer organic moiety and partly to the condensation of the residual hydrogen phosphate groups. The compositions of the diammonium-exchanged and the diamidated solids were determined by a combination of the thermogravimetric data for these solids and **1** (Table 1). The organic contents for the diamidated solids were

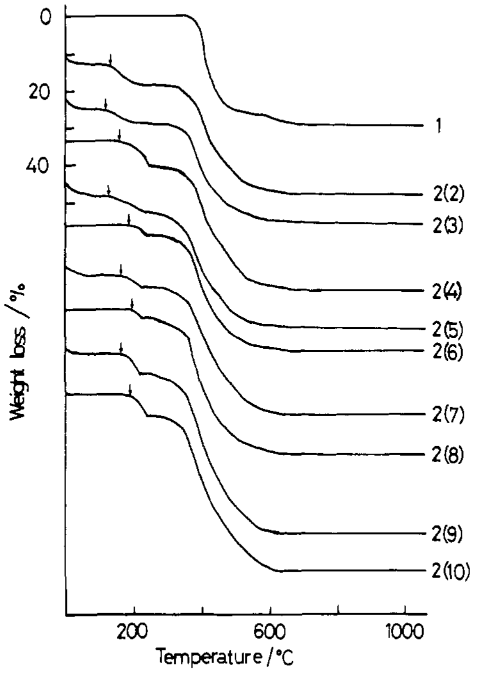

Figure 4. Thermogravimetric curves for **1** and **2**(*n*) with a heating rate of 10 °C min^{-1} in air. The vertical scales for **2**(*n*) are shifted by an arbitrary percentage.

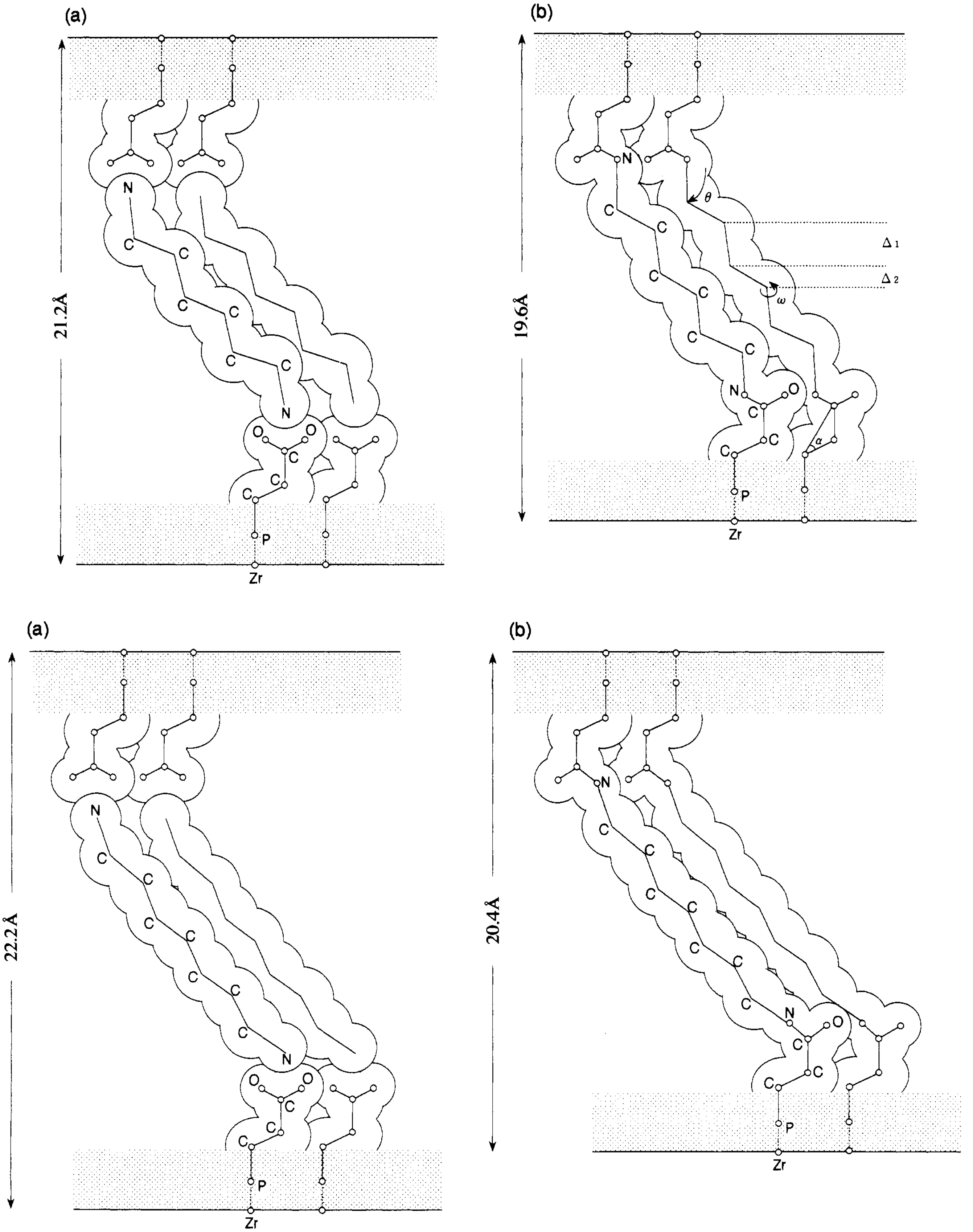

Figure 5. Models proposed for the arrangement of alkyl chains in the interlayer space of (a) the diammonium-exchanged and (b) the diamidated solids with (A, top) HeDA and (B, bottom) HpDA.

in fairly good agreement with those obtained from values of the third weight loss for the diammonium-exchanged solids. All the x values of 0.21–0.74 for the diammonium-exchanged solids are less than the upper limit of 1.67/2 or 0.835 expected from the composition of **1**. The x values of 0.21–0.41 for **2(3)**, **2(5)**, **2(6)**, **2(7)**, and **2(8)** are much less than 0.62–0.74 for the other diammonium-exchanged solids. The apparently low values for the former solids are due to the intercalated phases coexisting with the host phase remaining and/or any amorphous Zr-based phase such as $ZrO(OH)_2$. The partial decomposition of the host phase into such a dephosphorated phase was confirmed by X-ray data for PrDA and HeDA that showed the exchanged solids are converted into a mixture of ZrP_2O_7 and ZrO_2 upon heating at 1000 °C. These observations are consistent with additional X-ray data for PrDA, HeDa, and DeDA indicating that the interlayer spacing of intercalated phase is little affected by decreasing or increasing the [amine]/[Zr] mixing ratio from 1.0 to 0.5 or 2.0. In spite of the difference in reactivity, it is thus valid to compare the observed interlayer spacings for the intercalated phases formed at a fixed [amine]/[Zr] ratio of 1.0. It is also noticed that only the diammonium-exchanged solids with odd numbers of carbon atoms contain interlayer water desorbed at temperatures below 100 °C, except for EDA. This fact means that the intercalated alkyldiammonium ions with odd numbers of carbon atoms or very short carbon chain lengths would create an empty space large enough to include water molecules.

The slopes of the *d* vs *n* equations for the high and low chain-tilt forms of the diammoniated and the diamidated phosphonates yielded average angles of orientation between the carbon chains and the phosphonate layers on the assumption that the carbon planes are perpendicular to the layer, as described above. This assumption, however, is not always reasonable. So, we assumed that the intercalated alkyldiammonium or alkanediamide chains in all the phosphonates form a monomolecular layer with their fully extended alkyl chain axes tilted at an angle θ with respect to the zirconium phosphonate layers and with their carbon planes rotated at an angle ω around each chain axis, as illustrated for the diamidated form with HeDA in Figure 5A. The rotational angle ω is based on a value of 0° for a plane which is coplanar with the alkyl chain axis and perpendicular to the phosphonate layer. Then if the increases of interlayer spacing per CH_2 group for the rotation from odd to even and from even to odd numbers of methylene groups are denoted as Δd_1 and Δd_2, respectively, both quantities can be related to θ and ω by the equations

$$\Delta d_1 = r_0[(\cos\alpha)(\sin\theta) + (\sin\alpha)(\cos\theta)(\cos\omega)]$$

$$\Delta d_2 = r_0[(\cos\alpha)(\sin\theta) - (\sin\alpha)(\cos\theta)(\cos\omega)]$$

where r_0 is the C–C bond length or 1.54 Å and α is the angle between the C–C bond and the fully extended alkyl chain axis or 35.28°. The high chain-tilt groups of diammoniated and diamidated phases with $n \geq 6$ give the most reliable and sequential values of interlayer spacing. For these phases, the tilt angle θ_0 and the rotational angle ω_0 averaged over both rotations from even to odd and from odd to even were evaluated from $\theta_0 = \sin^{-1}[(\langle\Delta d_1\rangle + \langle\Delta d_2\rangle)/(2\cos\alpha)]$ and $\omega_0 = \cos^{-1}[(\langle\Delta d_1\rangle - \langle\Delta d_2\rangle)/(2\sin\alpha)(\cos\theta_0)]$, respectively. Here the $\langle\Delta d_1\rangle$ and $\langle\Delta d_2\rangle$ values were obtained by averaging each quantity Δd_1 or Δd_2 over all available rotations on the basis of the *d* values listed in Table 1. These calculations are summarized in Table 2. The large values of 80 and 72° for ω_0 indicate that the carbon planes in both forms are considerably rotated relative to the reference orientation. These rotational angles are also much more than 58° for the alkyldiammonium-exchanged form of α-ZrP evalauted from data in the literature[17] (Table 2).

Both ammonium termini of alkyldiammoniated molecules with their trans zigzag conformation are in trans and cis directions according to the even and odd numbers of carbon atoms, respectively. As suggested from the models given in Figure 5, therefore, the two ammonium termini of the diammoniated chains with even carbon numbers can rather easily be bound to the carboxyl groups of any two adjacent phosphonate layers, whereas either ammonium terminus of an odd carbon number chain cannot be brought into a position favorable for binding to any carboxyl group without changing its conformation. This explains the present observations that the diamines with even and odd carbon numbers generally produce the high and low chain-tilt forms, while those with even but short chains or odd but long ones yield both forms, due to their low or high chain flexibilities. The relatively low reactivity for OcDA to product the high chain-tilt form may result from a competition of the even and short chain effects. The chain deformation for the odd members would also result in such a porous structure as suggested from the water content data. The X-ray observations for the amidated phases suggest that the –CONH– groups covalently bonded to the phosphonate layers would restrict the chain flexibility, leading to the high and low chain-tilt forms depending only on the carbon chain length.

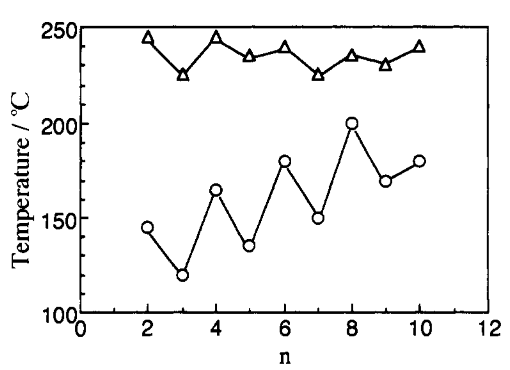

Figure 6. Plots of the (○) onset and (△) offset temperatures for the second weight loss in the thermogravimetric curves of **2**(*n*) as a function of carbon number.

Figure 6 shows the carbon number dependence of the onset and offset temperatures, T_{Gon} and T_{Goff}, for the second weight loss on the thermogravimetric curves for the diammonium-exchanged solids in Figure 4: T_{Gon} is indicated by an arrow on each curve. Some of the intercalated solids were heated at temperatures corresponding to each onset temperature for 10 min to yield IR spectra which indicate that the amidation with an accompanying deintercalation begins to occur at the onset temperature, as shown in Figure 3B. The onset temperature can therefore be characterized as a temperature at which the ammonium termini or the whole of the intercalated guest molecules are thermally mobilized to react with the nearby carboxyl groups or partly migrate out of the interlayer space. The increase in onset temperatures of ca. 8.9 °C per methylene unit for each even or odd carbon number group could be explained by assuming that the intercalated guest molecules with longer chain lengths are held in a more stable way in the interlayer space, due to the increased intermolecular attraction. The onset temperature exhibits another marked tendency to vary regularly up-and-down depending upon the even or odd numbers of carbon atoms. The offset temperature also shows the same odd/even effect, although the temperature is approximately constant over the whole range of *n*. For the odd carbon number phases, the porous structure formed after the desorption of water would make the alkyldiammonium ions more mobile, resulting in the formation of the amide form at relatively low temperatures. The exceptional behavior of EDA with a short chain length may be attributable to a strong attraction between the phosphonate layers which counteracts the molecular mobility enhanced by the porous structure. In contrast to the odd/even effect associated with guest components in the present system, similar but host-related effects were observed for the proton conductivity of carboxy-terminated zirconium phosphonates, $Zr(O_3P(CH_2)_nCOOH)_2$,[2a] and their reactivity toward both organic and inorganic guest molecules.[14]

Acknowledgment. The present work was supported by a Grant-in-Aid for General Scientific Research (05650843) from the Ministry of Education, Science, and Culture of Japan.

---

[17] (a) Casciola, M.; Costantino, U.; Dicroce, L.; Marmotti, F. *J. Inclusion Phenom.* **1988**, *6*, 291. (b) Costantino, U.; Marmottini, F. *Chim. Ind. (Milan)* **1988**, *70*, 93.